Eur. J. Wood Prod. (2015) 73:793–799
DOI 10.1007/s00107-015-0951-8

ORIGINAL

# Investigations into the influence of two different wood coatings on water diffusion determined by means of neutron imaging

**Walter Sonderegger[1] · Martin Glaunsinger[2] · David Mannes[3] · Thomas Volkmer[2] · Peter Niemz[1,2]**

Received: 17 September 2014 / Published online: 19 July 2015


**Abstract** The diffusion of water into spruce wood coated with an acrylate/polyurethane and with a silica-based coating system is investigated by varying the humidity conditions. Thereby, the change of moisture content (MC) is measured and analysed with the non-destructive method of neutron imaging. For the acrylate/polyurethane based coating system, the barrier effect of the coating on wood sorption in direct water contact and the influence of surface defects on this barrier effect are also tested. On changing the humidity conditions, the specimens with silica-based coating initially show a clear deceleration of the sorption process, whereas after 10 days the MC gradient is nearly similar to the uncoated reference specimens. In contrast, the specimens with acrylate/polyurethane based coating show a strong barrier effect against water sorption into wood over the whole measurement period when changing the humidity conditions and in direct water contact. As can be expected, a defect in the coating strongly reduces its barrier effect. Thereby, the kind of defect (saw kerf or blade cut) is rather irrelevant.

✉ Walter Sonderegger
wasonder@ethz.ch

[1] Institute for Building Materials (Wood Physics), ETH Zurich, Stefano-Franscini-Platz 3, 8093 Zurich, Switzerland

[2] Institute for Materials and Wood Technology, Bern University of Applied Sciences, Architecture, Wood and Civil Engineering, Solothurnstrasse 102, 2500 Biel, Switzerland

[3] Neutron Imaging and Activation Group (NIAG), Paul Scherrer Institute (PSI), 5232 Villigen PSI, Switzerland

## 1 Introduction

Wood coatings have a wide array of applications. In addition to their aesthetic contribution, they also show several protective characteristics. A major application of wood coating is to protect outdoor wood from direct water contact (rain, splash water) since wood with moisture content (MC) above 20 % is increasingly susceptible to insect and fungal attack. In addition, through the coating's barrier effect against water vapour, it diminishes the influence of ambient humidity changes on wood swelling and shrinkage. Depending on the composition, the barrier effect of the coating strongly varies. Thereby, solvent-borne coatings usually have a higher barrier effect than waterborne ones (De Meijer and Militz 2000; Van Meel et al. 2011). Furthermore, opaque coatings and coatings with darker pigmentation seem to be more durable than transparent or lightly pigmented ones and their durability increases with increasing film thickness (Grüll et al. 2014). Large problems may arise through stresses in the coating by swelling and shrinkage, which may result in coating failures (De Meijer and Militz 2000).

The aim of this paper is to investigate the influence of two different coating systems (acrylate/polyurethane and silica based) on the water vapour diffusion behaviour, the water uptake during direct water contact under the coating in the wood and the influence of surface defects. The moisture change within the wood over time was measured with the non-destructive neutron imaging method, which is an approved method in this research field and complements the nuclear magnetic resonance (NMR) technology (Pourmand et al. 2011; Van Meel et al. 2011), in order to determine the spatial distribution of MC changes (Lanvermann et al. 2014; Lehmann et al. 2001; Mannes et al. 2009; Sedighi-Gilani et al. 2012; Sonderegger et al. 2015).

## 2 Materials and methods

### 2.1 Material

For the tests, clear boards without knots, shakes or resin pockets and with a growth ring angle of about 45° and a mean density of 405 kg/m$^3$ at normal climate [20 °C/65 % relative humidity (RH)] from a stem of Norway spruce [*Picea abies* (L.) Karst.] from the region of Zurich, Switzerland were coated on one side with two different coating systems (Table 1) and one board was kept uncoated for reference measurements. Both coating systems were suitable for exterior application. System 1 was acrylate/polyurethane based and system 2 was silica based. The base coat and the finishing coat were each applied once for system 1 and twice for system 2 according to the manufacturer's data. The mean coating thickness was about 70 µm for system 1 and 180 µm for system 2.

Specimens sized 50 mm in the longitudinal (L) direction × 30 mm (height) × 10 mm (thickness) in the radial (R)—tangential (T) plane were cut from these boards for test 1, which evaluated water vapour diffusion at differential climate. Six specimens per coating system and per coating orientation (upper side, bottom side) as well as two reference specimens were used. For test 2, which investigated liquid water uptake and the influence of coating failures, the specimens (three specimens coated with system 1 and one reference specimen) were sized 50 mm (L) × 14 mm (height) × 10 mm (thickness). On two of the three specimens coated, artificial surface defects over the whole width were placed in the middle of the coated side of the specimen. These defects were made once with a saw kerf (thickness 3 mm) and once with a blade cut from a microtome (depth 0.5 mm), so that the coating was completely removed or cut through within the defected area. The specimens of both tests were conditioned at normal climate (20 °C/65 % RH) prior to the tests.

### 2.2 Methods

#### *2.2.1 Test 1: Water vapour diffusion at a differential climate*

The influence of the two coating systems on water vapour diffusion into the wood was tested. Therefore, in a similar manner to the cup-method described in ISO 12572 (2001), the specimens were exposed to a differential climate of 20 °C/65 % RH ambient environment (climate chamber) to almost 20 °C/100 % RH within the cup, which was filled with demineralised water up to about 15 mm below the bottom of the specimen (Fig. 1). The specimens were sealed with aluminium tape on four sides, leaving the upper and bottom side unsealed, so that diffusion only took place vertically upwards in the direction perpendicular to the coating and to the wood grain. In contrast to ISO 12572 (2001), where the water vapour diffusion or rather the water vapour resistance factor is to be determined at steady-state conditions, the water vapour diffusion into the wood at unsteady-state conditions (adsorption process) was analysed (Sonderegger et al. 2011). For this purpose, the method of neutron imaging offered the possibility to measure two-dimensionally the intrusion of absorbed water into the wood. To determine the water uptake of the specimens during the test, the specimens were neutron radiated at the beginning and also after 4 and 10 days, similar to the method by Sonderegger et al. (2010).

#### *2.2.2 Test 2: Liquid water uptake*

Test 2 investigated the barrier effect of coating system 1 against liquid water and the influence of coating failures. For the experiments, a specific specimen holder including a water container was built (Fig. 2). Each specimen was first sealed with aluminium tape on four sides similar to test 1 and then secured with screws between the upper and the lower part of the holder. Afterwards water was filled in the opening above the specimen. To prevent water outflow, the

**Table 1** Overview of the tested coating systems

| System (number) | Application | Type | Product | Basis | Colour |
|---|---|---|---|---|---|
| 1 | Interior and exterior | Base coat | AQUAPUR® Grip[a] | Acrylate/PU | White |
| | | Finishing coat | AQUASATIN® PU[a] | Acrylate/PU | White |
| 2 | Exterior (weatherproof)[c] | Base coat | KEIM Lignosil-Base[b] | Alkyd resin | Colourless |
| | | Finishing coat | KEIM Lignosil-Color[a] | Silica based | White |

*PU* Polyurethane

[a] Thinning with water

[b] Thinning with 10 % KEIM Lignosil-Base-DL

[c] Strongly waterproof but nevertheless water vapour permeable [SD < 0.5 m at wet-cup conditions according to ISO 12572 (2001)]

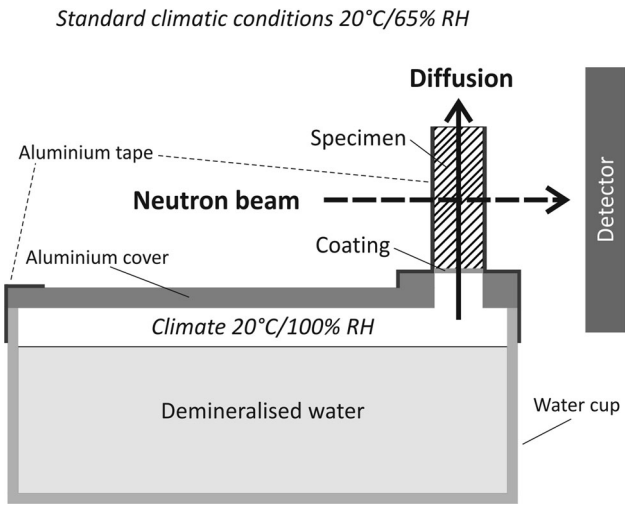


**Fig. 1** Schematic of experimental setup of test 1

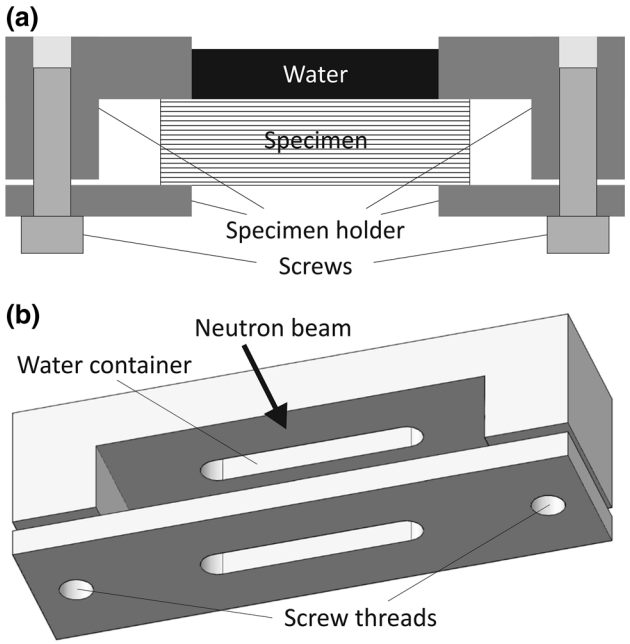


**Fig. 2** Setup of test 2: **a** profile, **b** 3-D view of the specimen holder

opening was smaller than the specimen and was sized 40 mm (length) × 6 mm (width). Similar to test 1, the water absorption of the wood was measured with the neutron imaging method. Neutron radiations were carried out over a period of 16 h (at the beginning and after 1, 4, 16 min and 1, 4, 16 h) in the direction perpendicular to the largest side of the specimen.

### 2.3 Evaluation

To evaluate and quantify the images from the neutron radiations, different correction procedures had to be performed. First, the images were corrected by the quantitative neutron imaging correction program QNI (Hassanein 2006) using dark current and flat field correction as well as median filtering (filter width: 3 pixels, threshold: 10 %). Further steps were carried out with the data processing program Fiji (Schindelin et al. 2012). The spots were cleaned by using the noise filter 'remove outliers'. The images of each series were cropped, rotated and aligned with the transformation specification 'Rigid Body' of the plugin 'StackReg' (Thévenaz et al. 1998) and then divided by the first image (obtained at the beginning of the test), so that only the water change during the test appears on the corrected image. To quantify the water concentration, an attenuation coefficient of $\Sigma_{water} = 2.2\ cm^{-1}$ was used according to Sonderegger et al. (2015). To convert the water concentration to the MC of the wood, the wood density from the first image was evaluated by means of an attenuation coefficient $\Sigma_{wood} = 1.88\ cm^{-1}$ (Mannes et al. 2009).

To evaluate the influence of the surface defects, depth profiles of the water uptake were calculated from three different regions of the sample: centre part, water head and total length (Fig. 3). From these profiles, the water absorption coefficient and the apparent diffusion coefficient from water absorption were calculated according to ISO 15148 (2002) and Klopfer (1974), respectively:

$$D^* = \left(\frac{A_w}{1.128 \cdot (c_2 - c_1)}\right) \quad (1)$$

with

$$A_w = \frac{\Delta m}{A \cdot \sqrt{t}}. \quad (2)$$

By converting Eq. 1, it corresponds to a useful form to determine the diffusion coefficient by the unsteady-state method in Siau (p. 150, 1995):

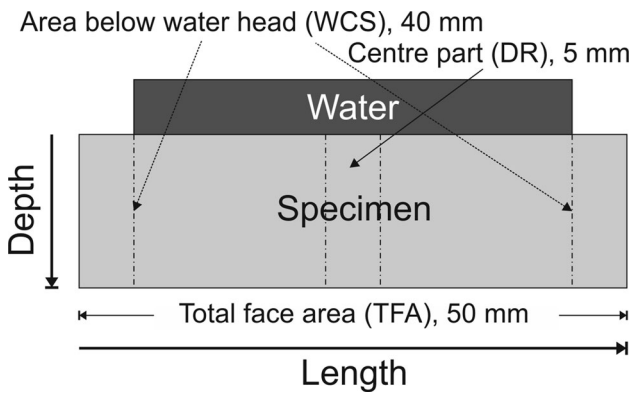


**Fig. 3** Test 2: Evaluated areas and directions of the specimen

$$D^* = \frac{(\bar{E})^2 \cdot L^2}{5.1 \cdot t} \quad (3)$$

where $D^*$ is the apparent diffusion coefficient ($m^2\ s^{-1}$), $A_w$ the water absorption coefficient ($kg\ m^{-2}\ s^{-0.5}$), $\Delta m$ the mass gain (kg), $A$ the face area ($m^2$), $t$ the time (s), $c$ the water concentration ($kg\ m^{-3}$) with $c_1$ the concentration of the test specimen at the beginning of the test (similar to 9 % MC) and $c_2$ the concentration at the upper side of the specimen during the test which is assumed to be similar to the fibre saturation point (FSP) at about 100 % RH (=30 % MC). $\overline{E}$ is the dimensionless average moisture concentration ($c–c_1/c_2–c_1$) and $L$ the length of a parallel sided specimen with sealed edges (diffusion occurs through the two opposite sides in an L-direction) or double length of a similar specimen with five sealed sides (thus, diffusion results only from one side).

## 3 Results and discussion

### 3.1 Test 1: Water vapour diffusion at a differential climate

The results of test 1 are presented in Fig. 4. They show the moisture distributions deduced and determined on the basis of the neutron images, relative to the height of the specimens exposed to a differential climate after 4 and 10 days. The sorption process had not yet reached the upper side of the specimens after 4 days in all of the variations. After 10 days, the moisture gradient through the reference specimens (uncoated) had reached the upper side and was already quite linear [about 85 % of the final state assuming a similar diffusion coefficient to test 2 (Table 2), cf. Klopfer 1974, p. 160]. Zwicker (2008) in Sonderegger et al. (2011) showed a similar MC gradient in the diffusion direction at final wet-cup test conditions (specimen thickness 20 mm, similar boundary conditions), also with a MC of about 25–26 % on the wet side of the specimens. The difference in MC on the wet specimen side to the MC at fibre saturation point (FSP) at 100 % RH, which corresponds to about 30 % MC, can be explained by a RH gradient in the air between the water in the cup and the bottom side of the specimen (cf. ISO 12572 (2001), appendix G).

The moisture distribution of the specimens coated at the top is quite similar to the reference specimens for both coating systems. This suggests that the sorption process is, in large part, unaffected by the conditions on the upper side of the specimen (cf. Klopfer 1974). For the final state, a higher MC at the top compared with the reference specimens is expected for the coated specimens due to the

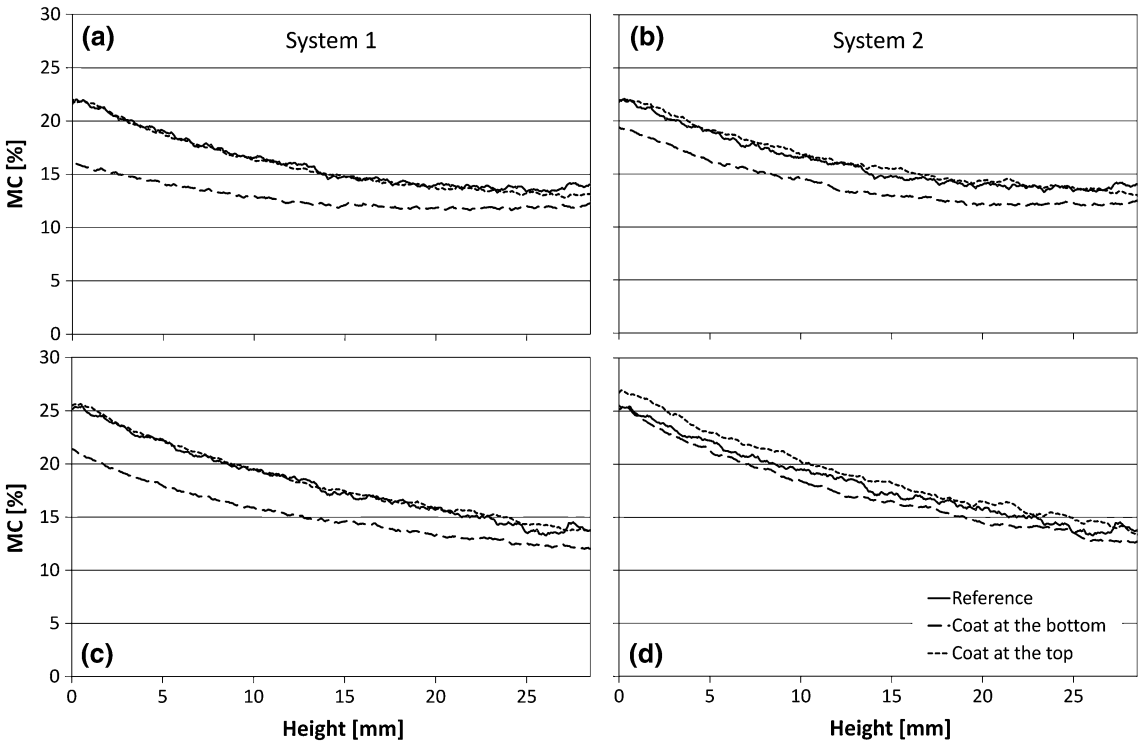


**Fig. 4** Test 1: Moisture distribution over specimen height after 4 days (**a**, **b**) and after 10 days (**c**, **d**) in a differential climate [20 °C/100 % RH (*left*) to 20 °C/65 % RH (*right*)], previously air-conditioned at normal climate (20 °C/65 % RH)

**Table 2** Water absorption coefficients ($A_w$) and thereof derived apparent diffusion coefficients (D*) calculated from values averaged over the total face area (TFA), over the water contact sector (WCS) and over the centre part near the damaged region (DR), cf. Fig. 3

| Coat system | Damage | $A_{w.TFA}$ (kg m$^{-2}$ s$^{-0.5}$) | $R^2$ | $A_{w.WCS}$ (kg m$^{-2}$ s$^{-0.5}$) | $R^2$ | $A_{w.DR}$ (kg m$^{-2}$ s$^{-0.5}$) | $R^2$ | $D^*_{TFA}$ (m$^2$ s$^{-1}$) | $D^*_{WCS}$ (m$^2$ s$^{-1}$) | $D^*_{DR}$ (m$^2$ s$^{-1}$) |
|---|---|---|---|---|---|---|---|---|---|---|
| 1 | – | 0.000021 | 0.89 | 0.000019 | 0.87 | – | – | 7.35 E−14 | 6.14 E−14 | – |
| 1 | Saw kerf | 0.000833 | 0.96 | 0.000874 | 0.96 | 0.00111 | 0.97 | 9.59 E−11 | 1.06 E−10 | 1.70 E−10 |
| 1 | Blade cut | 0.000944 | 0.986 | 0.00103 | 0.992 | 0.00128 | 0.99 | 8.67 E−11 | 1.02 E−10 | 1.58 E−10 |
| Reference (uncoated) | – | 0.00124 | 0.995 | 0.00126 | 0.995 | – | – | 1.77 E−10 | 1.83 E−10 | – |

$R^2$ coefficient of determination

barrier effect of the coating. Therefore, longer test duration should be advised in further experiments. Coated at the bottom, the acrylate/polyurethane based coating (system 1) shows a strong barrier effect after 4 and 10 days. The silica-based coating (system 2) also shows a clear deceleration of the sorption process after 4 days, whereas the MC gradient is nearly similar to the reference specimen after 10 days. This can be explained with a reduction of the barrier effect of the coating with increasing MC in such a way that the diffusion coefficient of the coating is similar to that of wood at high MC.

### 3.2 Test 2: Liquid water uptake

The results of test 2 are presented in Table 2 and Figs. 5, 6. In Table 2, the water absorption and diffusion coefficients calculated according to Eqs. 1 and 2 are listed from the different regions of the sample. The water absorption coefficient of the coated wood is about two orders of magnitude lower than that of the reference specimen, whether the values are averaged over the total face area ($A_{w.TFA}$) or only within the water contact sector ($A_{w.WCS}$). The corresponding apparent diffusion coefficients (influenced by the coating, wood and the interfacial layer between coating and wood) are even three orders of magnitude lower. Pourmand et al. (2011) measured a similar barrier effect only for an oil-based paint. In contrast, De Meijer and Militz (2000) measured clearly lower differences of the diffusion coefficients (factor $\geq$0.086) between coated spruce wood and uncoated samples over a period of 1700 h. Thus, the low diffusion coefficient of coating system 1, which included only the initial phase of the diffusion process, can be explained by the characteristic of water adsorption of coated wood, which is delayed in the initial phase according to Sivertsen and Flaete (2012) and therefore results in a too low apparent diffusion coefficient within this phase. If the water absorption values from test 1 after 4 and 10 days are considered, the barrier effect of the coating is clearly reduced to values similar to the measurements of De Meijer and Militz (2000).

For the reference specimen, the water absorption coefficient $A_{w.WCS}$ lies on the lower limit compared with measurements from Sonderegger (2011) and Niemz et al. (2010). In contrast, Sedighi-Gilani et al. (2012), who determined the water absorption coefficient also by means of the neutron imaging method, and some references in Niemz et al. (2010) clearly show (up to four times) higher values, which can be partly attributed to the different exposure times and partly to the high property variation within this species. Further, De Meijer and Militz (2000) determined two to five times higher diffusion coefficients.

The surface defects of the coating have a strong effect on the extent of water diffusion. Over the total face area, the barrier effect of the coating is strongly reduced and the diffusion coefficient increases to about half the value compared with that of the uncoated specimen. Thereby, the damage inflicted by utilising a blade shows only slightly lower diffusion coefficients than the damage inflicted through a saw. For the absorption coefficient, the values from the blade cut specimen are even higher due to its higher wood density. For the centre part, the values of the surface defected specimens are similar to the values of the reference specimen, which are illustrated in Fig. 5 where the MC profiles of the centre part are compared with those below the water sector. A profile along the length of the sample at 0.5 mm under the coating shows a clear MC increase in the defect region (Fig. 6).

## 4 Conclusion

The influence of two coating systems (acrylate/polyurethane and silica-based) and their barrier effect against water diffusion in wood, as well as the influence of coating failures, were tested with the neutron imaging method. Deduced from the neutron images, the moisture gradient

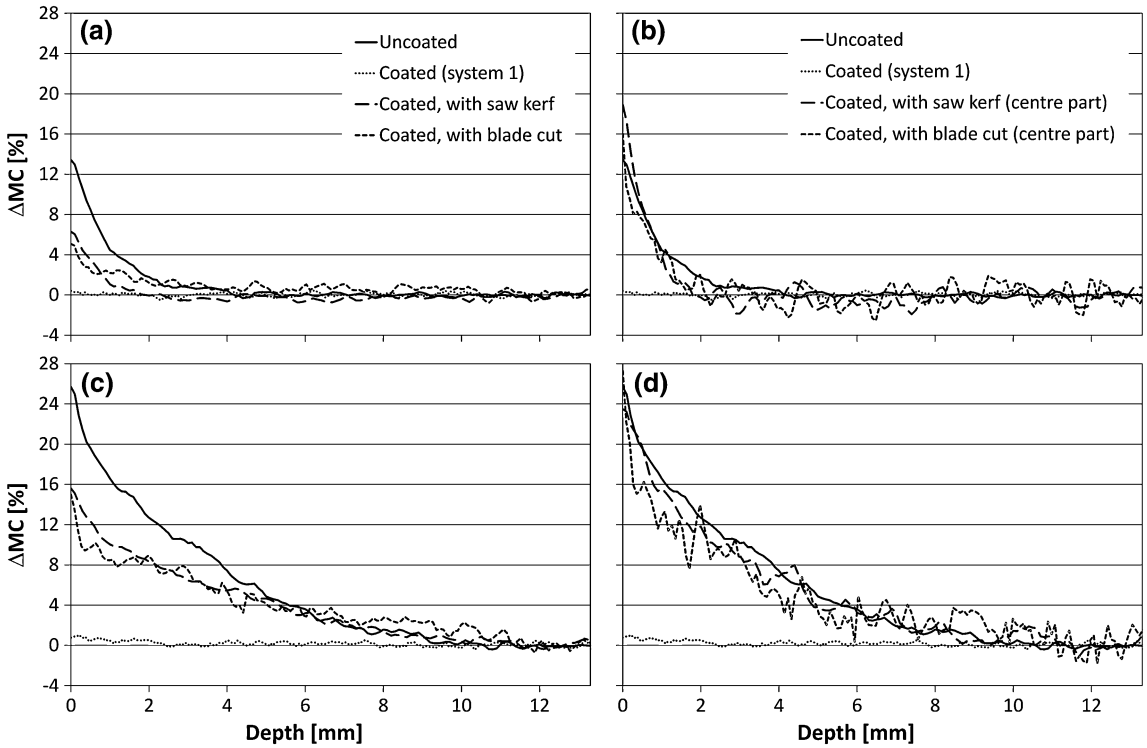


**Fig. 5** Test 2: Change of moisture content (ΔMC) after 1 h (**a**, **b**) and after 16 h (**c**, **d**). *Left* (**a**, **c**): mean values over the area below the water container; *right* (**b**, **d**): mean values of the centre part below the surface defects

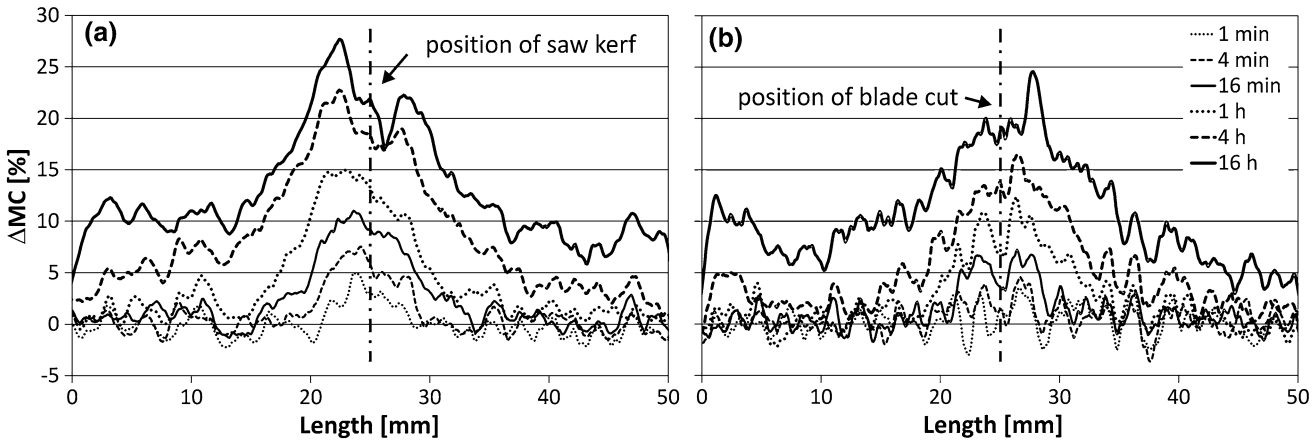


**Fig. 6** Test 2: Distribution of the moisture content increase (ΔMC) over the length of the two surface defected specimens with increasing time at 0.5 mm behind the coating; **a** specimen with saw kerf; **b** specimen with blade cut

through the wood specimens could be determined at different times and the water uptake near the coating failures could be quantified. When exposed to a differential climate, both the coating systems showed a clear deceleration in sorption after 4 days compared with the uncoated reference sample. Thereby the acrylate/polyurethane based coating had a stronger barrier effect than the silica-based coating. After 10 days, the latter is nearly congruent with the uncoated reference whereas the acrylate/polyurethane based coating still showed a clear sorption deceleration. The capacity of coating failures to reduce the barrier effect is evident. In a sector near the coating failure, the water uptake is similar to the uncoated specimen. The width of the failure only marginally influences the results.

**Acknowledgments** Thanks go to the Swiss Federal Office for the Environment (Fonds zur Förderung der Wald- und Holzforschung) for financial support.

## References

De Meijer M, Militz H (2000) Moisture transport in coated wood. Part 1: analysis of sorption rates and moisture content profiles in spruce during liquid water uptake. Holz Roh- Werkst 58(5):354–362

Grüll G, Tscherne F, Spitaler I, Forsthuber B (2014) Comparison of wood coating durability in natural weathering and artificial weathering using fluorescent UV-lamps and water. Eur J Wood Prod 72(3):367–376

Hassanein RK (2006) Correction methods for the quantitative evaluation of thermal neutron tomography. Dissertation, ETH Zurich

ISO 12572 (2001) Hygrothermal performance of building materials and products—Determination of water vapour transmission properties. International Organization for Standardization, Geneva

ISO 15148 (2002) Hygrothermal performance of building materials and products—Determination of water absorption coefficient by partial immersion. International Organization for Standardization, Geneva

Klopfer H (1974) Wassertransport durch Diffusion in Feststoffen. (Water transport through diffusion in solids) Bauverlag, Wiesbaden/Berlin **(in German)**

Lanvermann C, Sanabria SJ, Mannes D, Niemz P (2014) Combination of neutron imaging (NI) and digital image correlation (DIC) to determine intra-ring moisture variation in Norway spruce. Holzforschung 68(1):113–122

Lehmann E, Vontobel P, Scherrer P, Niemz P (2001) Application of neutron radiography as method in the analysis of wood. Holz Roh- Werkst 59(6):463–471 **(in German)**

Mannes D, Josic L, Lehmann E, Niemz P (2009) Neutron attenuation coefficients for non-invasive quantification of wood properties. Holzforschung 63(4):472–478

Niemz P, Mannes D, Koch W, Herbers Y (2010) Investigations into the water absorption coefficients of timber with variations in timber and moisture type. Bauphysik 32(3):149–153 **(in German)**

Pourmand P, Wang L, Dvinskikh SV (2011) Assessment of moisture protective properties of wood coatings by a portable NMR sensor. J Coat Technol Res 8(5):649–654

Schindelin J, Arganda-Carreras I, Frise E, Kaynig V, Longair M, Pietzsch T, Preibisch S, Rueden C, Saalfeld S, Schmid B, Tinevez J-Y, White DJ, Hartenstein V, Eliceiri K, Tomancak P, Cardona A (2012) Fiji: an open-source platform for biological-image analysis. Nat Methods 9(7):676–682

Sedighi-Gilani M, Griffa M, Mannes D, Lehmann E, Carmeliet J, Derome D (2012) Visualization and quantification of liquid water transport in softwood by means of neutron radiography. Int J Heat Mass Tran 55(21–22):6211–6221

Siau JF (1995) Wood: Influence of moisture on physical properties. Virginia Polytechnic Institute and State University, USA

Sivertsen MS, Flaete PO (2012) Water absorption in coated Norway spruce (*Picea abies*) cladding boards. Eur J Wood Prod 70(1–3):307–317

Sonderegger W (2011) Experimental and theoretical investigations on the heat and water transport in wood and wood-based materials. Dissertation, ETH Zurich

Sonderegger W, Hering S, Mannes D, Vontobel P, Lehmann E, Niemz P (2010) Quantitative determination of bound water diffusion in multilayer boards by means of neutron imaging. Eur J Wood Prod 68(3):341–350

Sonderegger W, Vecellio M, Zwicker P, Niemz P (2011) Combined bound water and water vapour diffusion of Norway spruce and European beech in and between the principal anatomical directions. Holzforschung 65(6):819–828

Sonderegger W, Mannes D, Kaestner A, Hovind J, Lehmann E (2015) On-line monitoring of hygroscopicity and dimensional changes of wood during thermal modification by means of neutron imaging methods. Holzforschung 69(1):87–95

Thévenaz P, Ruttimann UE, Unser M (1998) A pyramid approach to subpixel registration based on intensity. IEEE T Image Process 7(1):27–41

Van Meel PA, Erich SJF, Huinink HP, Kopinga K, de Jong J, Adan OCG (2011) Moisture transport in coated wood. Prog Org Coat 72(4):686–694

Zwicker P (2008) Untersuchungen zum Diffusionsverhalten von Holz und Holzwerkstoffen. (Investigations into the diffusion behavior of wood and wood based products) Bachelor thesis, Institute for Building Materials (Wood Physics), ETH Zurich **(in German)**